Vision Research 49 (2009) 2518–2530

Contents lists available at ScienceDirect

Vision Research

journal homepage: www.elsevier.com/locate/visres

Curvature coding in illusory contours

Elena Gheorghiu *, Frederick A.A. Kingdom, Manpreet Sull, Samantha Wells

McGill Vision Research, Department of Ophthalmology, McGill University, 687 Pine Avenue W., Montreal, Quebec, Canada H3A 1A1

ARTICLE INFO

Article history:
Received 27 March 2009
Received in revised form 17 June 2009

Keywords:
Illusory contours
Curvature
Adaptation
After-effect
Polarity
Scale
Orientation

ABSTRACT

We have employed the shape frequency and shape-amplitude after-effects (SFAE and SAAE) to investigate: (i) whether the shapes of illusory and real curves are processed by the same or different mechanisms, and (ii) the carrier-tuning properties of illusory curvature mechanisms. The SFAE and SAAE are the phenomena in which adaptation to a sinusoidal-shaped contour results in a shift in, respectively, the perceived shape-frequency and perceived shape-amplitude of a test contour in a direction away from that of the adapting stimulus. Both after-effects are believed to be mediated by mechanisms sensitive to curvature (Gheorghiu & Kingdom, 2007a, 2009; see also Hancock & Peirce, 2008). We observed both shape after-effects in sinusoidally-shaped illusory contours defined by phase-shifted line-grating carriers. We tested whether illusory and real contours were mediated by the same or different mechanisms by comparing same adaptor-and-test with different adaptor-and-test combinations of real and illusory contours. Real contour adaptors produced after-effects in illusory contour tests that were as great as, or even greater than those produced by illusory contour adaptors. However, illusory contour adaptors produced much weaker after-effects in real contour tests than did real contour adaptors. This asymmetry suggests that illusory contour curves are encoded by a sub-set of mechanisms sensitive to real contour curves. We also examined the carrier-tuning properties of illusory-contour curvature processing using adaptor and test illusory contours that differed in the luminance contrast-polarity, luminance scale and orientation of the carriers. We found no selectivity to any of these dimensions for either even-symmetric or odd-symmetric line-gratings carriers, even though selectivity to these dimensions was found for real contours.

1. Introduction

Two phase-shifted abutting line gratings (see Fig. 1) can elicit a strong percept of a sine-wave-shaped illusory contour, or IC, even though the average luminance on either side of the boundary is the same. The line gratings that support the illusory contour in Fig. 1 are termed the 'carrier'.

Numerous psychophysical studies have suggested that ICs play a similar role in vision to real contours, or RCs. For example, ICs exhibit the tilt after-effect (Paradiso, Shimojo, & Nakayama, 1989; Smith & Over, 1975, 1977, 1979; van der Zwan & Wenderoth, 1995), are subject to orientation masking (Berkley, Debruyn, & Orban, 1994; Halpern, Salzman, Harrison, & Widaman 1983; Tyler, 1975) and show good orientation discrimination (Vogels & Orban, 1987), suggesting that ICs are involved in coding orientation. Illusory contours support apparent motion (Ramachandran, 1986; von Grunau, 1979) and elicit the motion after-effect (Smith & Over, 1979), suggesting also a role in motion processing. Illusory contours also exhibit good vernier acuity (Greene & Brown, 1997), suggesting a role in position and/or orientation coding.

In this communication we begin by demonstrating that ICs play a role in the coding of curvature. We demonstrate that ICs exhibit two shape after-effects previously demonstrated in RCs and shown to be mediated by curvature-sensitive mechanisms. The two shape after-effects are the shape-frequency and shape-amplitude after-effects, or SFAE and SAAE (Gheorghiu & Kingdom, 2007a, 2007b, 2008, 2009; Gheorghiu, Kingdom, Thai, & Sampasivam, 2009). These after-effects are the perceived shifts in, respectively, the shape-frequency and shape-amplitude of a sine-wave-shaped contour following adaptation to a sine-wave-shaped contour of slightly different shape-frequency/shape-amplitude. Readers may experience the SFAE and the SAAE with ICs in Fig. 1a and b, by first moving their eyes back and forth along the horizontal markers on the left for about a minute, and then transferring their gaze to the central spot on the right. The two test illusory contour-shapes, which are physically identical, should appear different in shape-frequency or shape-amplitude. Both after-effects survive shape-phase randomization during adaptation, as can be experienced in the RC non-static-adaptor versions on http://www.mvr.mcgill.ca/Fred/research.htm#contourShapePerception. In the experiments

* Corresponding author.
E-mail address: elena.gheorghiu@mcgill.ca (E. Gheorghiu).

0042-6989/$ - see front matter © 2009 Elsevier Ltd. All rights reserved.
doi:10.1016/j.visres.2009.08.009

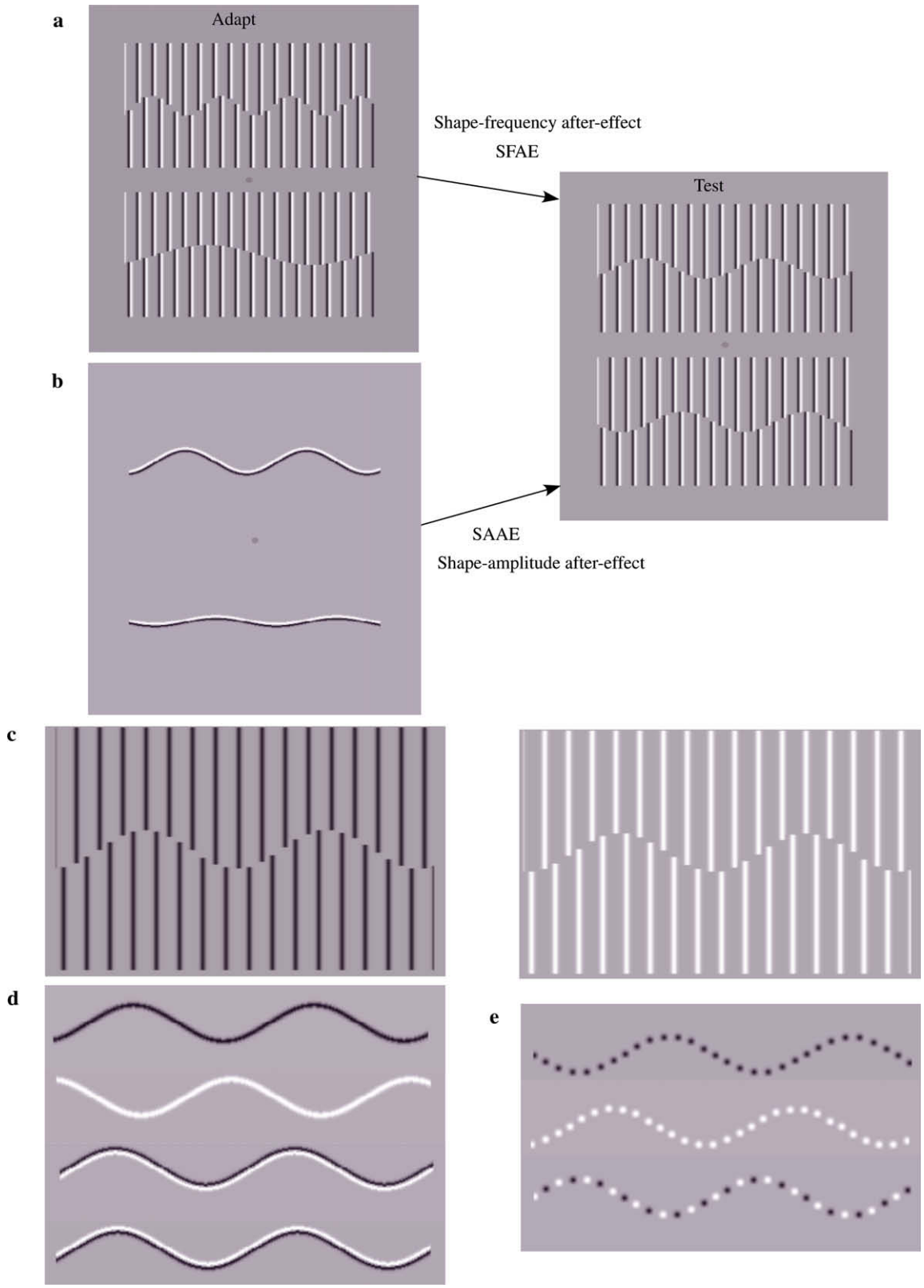

Fig. 1. Illusory contours (ICs) and real contours (RCs) used in the experiments. One can experience: (a) the shape-frequency after-effect (SFAE) and (b) the shape-amplitude after-effect (SAAE) by moving one's eyes back and forth along the markers located midway between the pair of adapting contours (left) for about 90 s, and then shifting one's gaze to the middle of the test contours (right). Example stimuli: (c) ICs constructed from even-symmetric line-grating carriers whose contrast polarity was either 'bright' (right panel) or 'dark' (left panel). (d) Even- and odd-symmetric RCs whose contrast polarity was either dark, bright, dark-bright and bright-dark. (e) RCs constructed from Gaussian-blobs, either 'dark', 'bright' or 'alternating bright and dark'.

described below we show comparable-sized SFAEs and SAAEs for ICs and RCs.

Having demonstrated that ICs are involved in the coding of curvature, we consider two questions: first, are IC and RC curves coded by the same mechanisms, and second, are IC curvature mechanisms selective for different types of carrier?

With regard to the first question, what might the literature lead us to expect? Paradiso et al. (1989) found only a small amount of transfer of the tilt after-effect between IC adaptors and RC tests, suggesting that the coding of orientation in RCs and ICs is primarily mediated by different mechanisms. On the other hand, Berkley et al. (1994) reported strong transfer of the tilt after-effect between ICs and RCs. Although they used similar stimuli to that of Paradiso et al. (1989), the after-effects were only obtained when the stimuli were degraded by the addition of static noise. To our knowledge no psychophysical studies have examined whether the shapes of ICs and RCs are processed by a common mechanism.

Single-unit recordings have shown that neurons in V1 and V2 respond to both RCs and ICs (Peterhans & von der Heydt, 1989; Vogels & Orban, 1987; Von der Heydt & Peterhans, 1989; Grosof, Shapley, & Hawken, 1993; Lee & Nguyen, 2001; Von der Heydt, Peterhans, & Baumgartner, 1984), with stronger responses to ICs in V2 than V1. However, beyond V2 it is not known whether neurons respond to both ICs and RCs. A single study by Sary et al. (2007) explored the shape-sensitivity of IT neurons to ICs and RCs. They found that most IT neurons were responsive to both IC and RC shapes but that the average firing rate was significantly lower and the response latency significantly longer for the IC shapes. Sary et al. (2007) concluded that the response characteristics of IT neurons was different for RC shapes that were defined by surface structure and color, compared to IC shapes, but similar for silhouettes of RC shapes and IC shapes. This suggests an invariance to shapes defined solely by contours but lacking internal surface information. Brain imaging (fMRI) studies in humans indicate that ICs activate intermediate-to-high (V3, V4, V7, LO) and low (V1 and V2) visual areas (Ffytche & Zeki, 1996; Hirsch et al., 1995; Mendola, Dale, Fischl, Liu, & Tootell, 1999; Montaser-Kouhsari, Landy, Heeger, & Larsson, 2007), all of which are known to be activated by RCs. However, lesion studies in V4 (De Weerd, Desimone, & Ungerleider, 1996; Merigan, 1996) and IT of macaque monkeys (Huxlin, Saunders, Marchionini, Pham, & Merigan, 2000) have shown that while IC shape discrimination is severely impaired, RC shapes and IC shapes with an added outline are not. Taken together, neurophysiological, brain imaging and lesion studies do not converge on a consensus as to whether IC and RC shapes are processed by a common mechanism.

What of the second question, namely whether IC curvature mechanisms are carrier-selective? A number of psychophysical studies have investigated the effects of carrier luminance-contrast-polarity, carrier luminance-scale and carrier orientation on the perception of ICs. These studies used ICs with phase-shifted line-grating carriers (Dresp, Salvano-Pardieu, & Bonnet, 1996; Soriano, Spillman, & Bach, 1996), phase-shifted concentric rings (Berkley et al., 1994; Lesher & Mingolla, 1993; Paradiso et al., 1989), or circular ICs with carriers only outside the circle (He & Ooi, 1998; Prazdny, 1983). The carriers in these studies consisted of either black, white or alternating black and white lines on a grey or white background. He and Ooi (1998) reported stronger impressions of ICs when the carrier elements had the same as opposed to alternating contrast polarity, suggesting a degree of selectivity to carrier contrast polarity. However, Prazdny (1983) reported strong percepts of ICs from carriers whose lines alternated in contrast polarity, and Dresp et al. (1996) reported stronger ICs and shorter response times for alternating compared to same contrast polarity carriers. However, Dresp et al. also showed that when the contrast within a carrier line alternated, ICs were not perceived. Single-unit recordings (Baumann, van der Zwan, & Peterhans, 1997; Peterhans & Heitger, 2001) have shown that only a small minority of IC-responsive neurons in V2 are sensitive to contrast polarity. Taken together, these studies concerning the carrier contrast-polarity tuning properties of IC perception suggest that IC mechanisms are to some extent sensitive to carrier contrast polarity. However, because no study has measured shape coding in ICs, it remains unresolved as to whether IC curvature mechanisms are selective for carrier contrast polarity.

With regard to the spatial dimensions of the carrier, several studies have reported that line width has an effect on the saliency of ICs (Lesher & Mingolla, 1993; Petry, Harbeck, Conway, & Levey, 1983; Soriano, Spillmann, & Bach, 1996). Soriano et al. (1996), using carriers consisting of black lines on a white background, showed that when line width was increased while holding the duty cycle constant, the impression of an IC decreased slightly. Once again however no study has investigated whether illusory-based shape mechanisms are selective to the spatial dimensions of the carrier.

Finally, with regard to carrier orientation, a number of studies have shown that impressions of ICs can be obtained with carriers that are not oriented orthogonally to the IC, as with curved or slanted carriers (Montaser-Kouhsari et al., 2007; Parks, 1980; Wilson & Richards, 1992). However, Soriano et al. (1996) found that IC strength decreased with an increase in the angle of one line grating relative to the other, once the angle exceeded 20°. Soriano et al. also reported that when the ICs were rotated as a whole, vertical ICs were stronger than horizontal ICs, and both vertical and horizontal ICs were stronger than ICs of intermediate orientations. The lowest rating strength for ICs was obtained at 45°, indicating that ICs undergo an oblique effect. The decrease in strength of ICs when the carriers are oblique rather than orthogonal to the IC border has also been found with single-unit recordings (von der Heydt & Peterhans, 1989). Once again, no psychophysical or neurophysiological studies have investigated whether IC shape mechanisms are selective to carrier orientation.

In order to address these questions we have investigated whether: (i) SFAEs and SAAEs obtained with IC adaptors transfer to RC tests and vice versa, and whether (ii) SFAEs and SAAEs obtained with IC adaptors of particular carrier luminance-contrast-polarity, luminance scale and orientation, transfer to IC tests of a different carrier luminance-contrast-polarity, luminance scale and orientation. We used sinusoidally-shaped illusory contours (see Fig. 1) whose carriers were lines with either odd- or even-symmetric luminance profiles.

2. General methods

2.1. Observers

Four subjects participated in the study. All subjects had normal or corrected-to-normal visual acuity. Each subject gave informed consent prior to participation in accordance with the university guidelines.

2.2. Stimuli

The stimuli were generated by a VSG2/5 video-graphics card (Cambridge Research Systems) with 12-bits contrast resolution, presented on a calibrated, gamma-corrected Sony Trinitron monitor, running at 120 Hz frame rate and with a spatial resolution of 1024×768 pixels. The mean luminance of the monitor was 42 cd/m^2.

Adaptation and test stimuli consisted of pairs of either sine-wave-shaped illusory contours or sine-wave-shaped real contours.

Example RCs and ICs are shown in Fig. 1. The stimuli were presented in the center of the monitor on a uniform grey background with a luminance of 42 cd/m^2. Each contour filled an area 8 (width) × 4 (height) deg. The IC carriers were vertical line gratings with a duty cycle of 0.5°. ICs were created by a relative shift in carrier phase of half the line separation, i.e. 0.25°. Unless otherwise stated, the adaptor pair for the SFAE consisted of contours with a shape-amplitude of 0.4° and shape frequencies of 0.15 and 0.45 c/deg, giving a geometric mean shape-frequency of 0.26 c/deg. For the SAAE, the shape-frequency of the adaptor pair was 0.4 c/deg, while the shape-amplitudes were 0.15 and 0.45°, giving a geometric mean shape-amplitude of 0.26°. The two adaptors and tests were presented 3.5° above and below the fixation marker. The cross-sectional luminance profiles of the RCs and of the IC carriers were of two types: odd- and even-symmetric. In all experiments the IC carrier lines and RCs had an odd-symmetric luminance profile except in Experiment 2 in which both odd- and even-symmetric profiles were used. Even-symmetric profiles (Fig. 1c) were generated according to a Gaussian function:

$$L(d) = L_b \pm L_b \cdot C \cdot \exp[-(d^2)/(2\sigma^2)] \quad (1)$$

where d is the distance from the center of the contour in a direction perpendicular to the tangent, L_b background luminance of 42 cd/m^2, C contrast and σ the space-constant, or standard deviation, that determines the width of the contour. The ± sign determined the polarity of the Gaussian (bright or dark). Odd-symmetric profiles (Fig. 1a and f) were generated according to a first derivative (1D) of a Gaussian function:

$$L(d) = L_b \pm L_b \cdot C \cdot \exp(0.5) \cdot (d/\sigma) \cdot \exp[-(d^2)/(2\sigma^2)] \quad (2)$$

where d, L_b, C and σ are as defined above. Unless otherwise stated, contrast C was set to 0.85 and σ to 0.04°. The ± sign determined the polarity of the contour. The term exp(0.5) gives the profile the same peak, or trough value as the Gaussian function in Eq. (1). Our RCs were designed to have a constant cross-sectional width, and the method used to achieve this is described in Gheorghiu and Kingdom (2006).

2.3. Procedure

Each session began with an initial adaptation period of 90 s, followed by a repeated test of 0.5 s duration interspersed with top-up adaptation of 2.5 s. During the adaptation period, the shape-phase of the RCs and ICs was randomly changed every 0.5 s in order to prevent the formation of afterimages and to minimize any effects of local orientation adaptation. The presentation of the test contour was signaled by a tone. The shape-phase of the test contour was also randomly assigned in every test period. The IC carriers were static and only the shape-phase of the IC itself was randomly changed. The display was viewed in a dimly lit room at a viewing distance of 100 cm. Subjects were required to fixate on the marker placed between each pair of contours for the entire session. A head and chin rest helped to minimize head movements.

A staircase method was used to estimate the PSE. For the SFAE the geometric mean shape-frequency of the two test contours was held constant at 0.26 c/deg while the computer varied the relative shape-frequencies of the two tests in accordance with the subject's response. At the start of the test period the ratio of the two test shape-frequencies was set to a random number between 0.7 and 1.44. On each trial subjects indicated via a button press whether the upper or lower test contour had the higher perceived shape-frequency. The computer then changed the ratio of test shape-frequencies by a factor of 1.06 for the first five trials and 1.015 thereafter, in a direction opposite to that of the response, i.e. towards the point of subjective equality (or PSE). The session was terminated after 25 trials. In order that the total amount of adaptation for each condition was the same, we used a staircase method that was terminated after a fixed number (25) of trials, rather than a fixed number of reversals. We found in pilot studies that 25 trials were as a rule sufficient to produce a convergence that was stable over the last 20 trials. The shape-frequency ratio at the PSE was calculated as the geometric mean shape-frequency ratio of the test that followed the lower shape-frequency adaptor to the test that followed the higher shape-frequency adaptor, averaged across the last 20 trials. For each with-adaptor condition we made six measurements, three in which the upper adaptor had the higher shape-frequency and three in which the lower adaptor had the higher shape-frequency. In addition we measured for each condition the shape-frequency ratio at the PSE in the absence of the adapting stimulus (i.e. the no-adaptor condition). To obtain an estimate of the size of the SFAE we first calculated the difference between the logarithm of each with-adaptor shape-frequency ratio at the PSE and the mean of the logarithms of the no-adaptor shape-frequency ratios at the PSE. We then calculated the mean and standard error of these differences across the six measurements, and these are the values shown in the graphs.

The procedure for measuring the SAAE followed the same principle as for the SFAE. The computer varied the relative shape-amplitudes of the two tests in accordance with the subject's response, while the geometric mean shape-amplitude of the two test contours was held constant at 0.26°.

3. Experiments and results

3.1. Experiment 1: interaction between illusory and real contours in the SFAE and SAAE

We begin by considering: (a) whether adaptation to sine-wave-shaped ICs produces SFAEs and SAAEs comparable to those obtained with RCs, and (b) how much transfer of the after-effects there is from ICs to RCs and vice versa. There were two conditions: (i) same adaptor and test, either RCs or ICs, and (ii) different adaptor and test, i.e. IC-adaptor/RC-test, and vice versa. The magnitude of transfer was defined as the log shape-frequency (or shape-amplitude) ratio obtained under the different adaptor condition divided by the log shape-frequency (or shape-amplitude) ratio obtained under the same adaptor-test condition.

Fig. 2 shows SFAEs and SAAEs for same adaptor and test conditions, both IC and RC (white bars), and different adaptor and test conditions: IC-adaptor/RC-test (dark gray bars) and RC-adaptor/IC-test (light gray bars). The results show that SFAEs/SAAEs are: (i) slightly lower in most subjects for IC compared to RC contours (compare white bars in Fig. 2); (ii) prominently reduced for IC-adaptors/RC-tests; (iii) larger for RC-adaptors/IC-tests (compare dark and light gray bars).

Fig. 3 shows the amount of transfer of after-effect between the two types of contours for the SFAE (Fig. 3a) and SAAE (Fig. 3b). The illusory-to-real transfer was calculated as the magnitude of the after-effect obtained with an IC-adaptor/RC-test divided by the magnitude of the after-effect obtained with an RC-adaptor/RC-test (dark gray bars in Fig. 3). The real-to-illusory transfer was calculated as the magnitude of the after-effect obtained with an RC-adaptor/IC-test divided by the magnitude of the after-effect obtained with an IC-adaptor/IC-test (light gray bars in Fig. 3). Note that the transfer in both instances is measured in terms of the relative effect of different adaptors on the same test, rather than the relative effect of the same adaptor on different tests. This rule of comparing after-effects from different adaptors on the same test is adopted throughout the analyses presented here, unless otherwise specified. A transfer value of 1 indicates that the magnitude

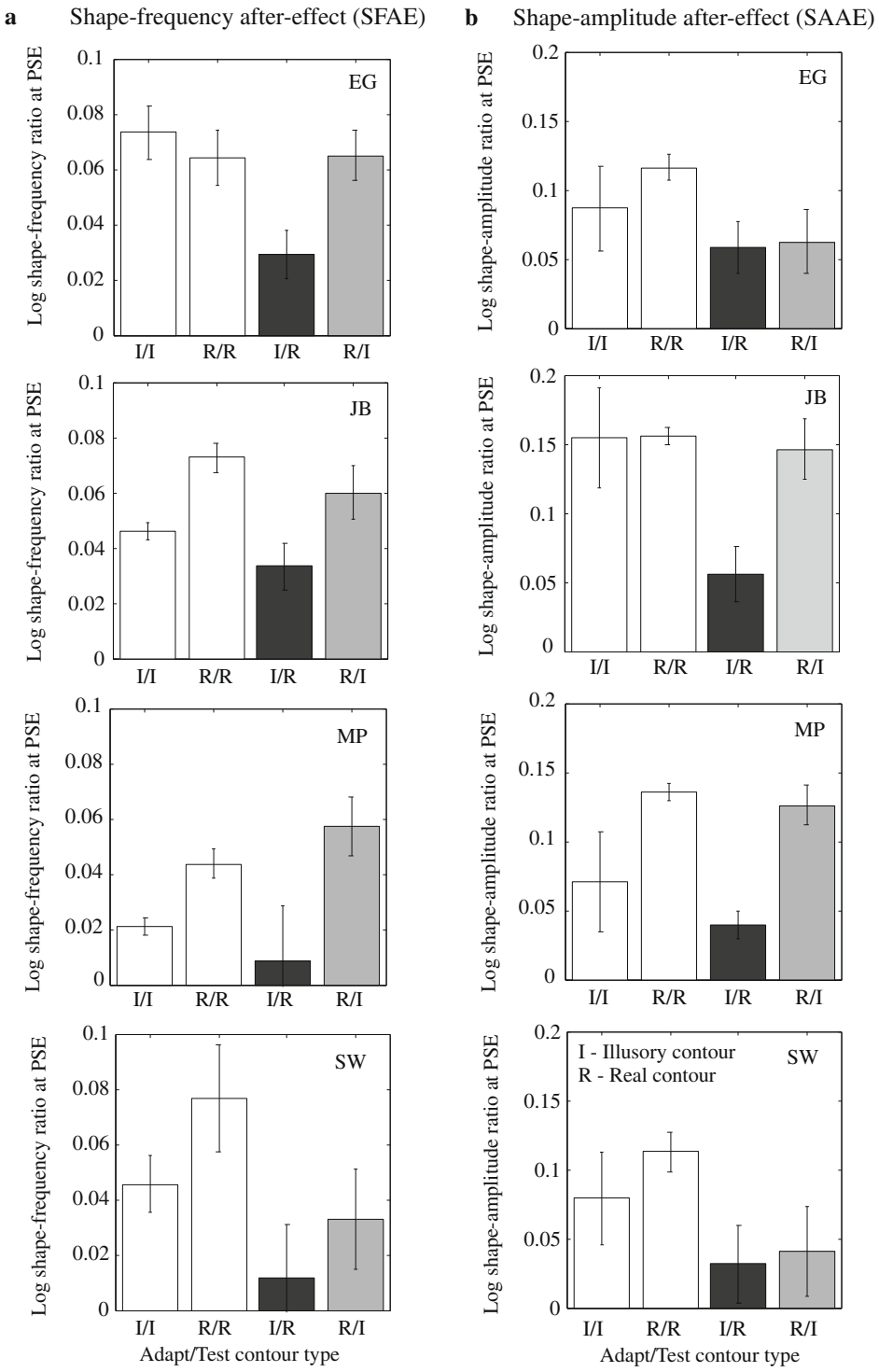

Fig. 2. Results for Experiment 1: (a) SFAEs and (b) SAAEs for same adaptor and test conditions, either IC or RC (white bars), and different adaptor and test conditions, either IC adaptor and RC test (dark gray bars), or RC adaptor and IC test (light gray bars). Error bars represent standard errors of the mean difference between the with-adaptor and no-adaptor conditions calculated across six measurements.

of the after-effect obtained in the different and same adaptor-test conditions are the same. The results indicate a strong asymmetry in transfer between illusory-to-real and real-to-illusory contours. Also, two subjects (JB and MS) show larger after-effects with RC-adaptors/IC-tests than with IC-adaptors/IC-tests (compare light gray bars with the dashed line in Fig. 3). For both after-effects, all four subjects show large transfer from real-to-illusory and reduced transfer from illusory-to-real (compare light and dark gray bars in Fig. 3). On average, the transfer from real-to-illusory contours was 1.4 for SFAE and 0.99 for SAAE, and from illusory-to-real contours 0.31 for SFAE and 0.35 for SAAE.

In a previous study, Gheorghiu and Kingdom (2006) showed that the SFAEs obtained with RCs were relatively invariant to the contrast of either adaptor or test. They did however find that SFAEs were largest when adaptor and test were equal in contrast. In the present experiment, in which we examined illusory-to-real trans-

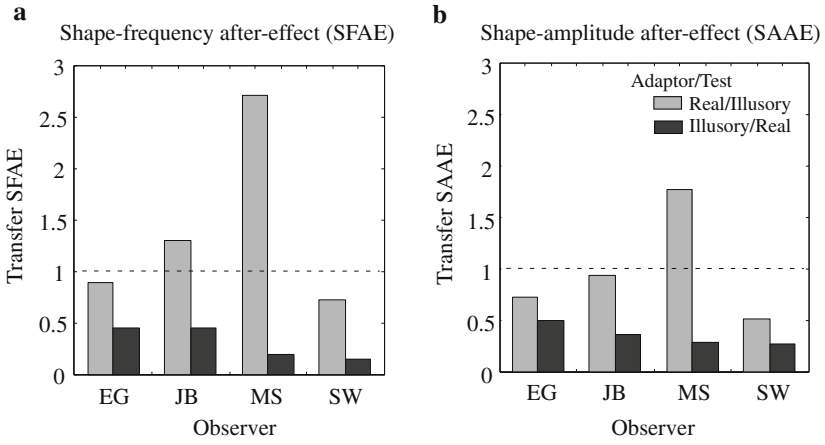

Fig. 3. Transfer of SFAE: (a) and SAAE (b) from real-to-illusory (light gray bars) and illusory-to-real (dark gray bars) contours. The amount of transfer was defined as the log shape-frequency (or shape-amplitude) ratio obtained under the different adaptor/test condition divided by the log shape-frequency (or shape-amplitude) ratio obtained under the same adaptor/test condition, where the same adaptor/test condition employed the test contour-type used in the different adaptor/test condition. The rule of comparing after-effects from different adaptors with the same test is adopted throughout the analyses presented here. A transfer value of 1 indicates that the magnitude of the after-effect obtained in the different and same adaptor/test conditions is the same.

fer, it is possible that the prominent reduction in the after-effect using an IC-adaptor/RC-test occurred because the IC adaptor had a lower effective contrast than the RC test. To test this possibility we lowered the contrast of the RC test to one of three contrast values: 0.1, 0.29 and 0.85. If the difference in effective contrast between an IC-adaptor/RC-test caused the reduction in the after-effects in Fig. 3 (dark gray bars), we should expect an increase in the size of the after-effect with a lower contrast RC test.

Fig. 4 shows the results. The dashed lines indicate the size of the after-effect obtained using the RC adaptor from the first experiment: thick dashed lines for the RC test and thin dashed lines for the IC test. Fig. 4 shows that irrespective of the RC test contrast, the after-effects with IC adaptors are still prominently lower than those obtained using RC adaptors and tests (compare the size of the light gray bars with the thick dashed line). They are also lower than those obtained from RC-adaptors/IC-tests (compare the size of the light gray bars with the thin dashed line). This indicates that the difference in the transfer of after-effect between real-to-illusory and illusory-to-real contours is not due to the reduced effective contrast of the IC adaptors.

3.2. Experiment 2: effect of luminance contrast-polarity

In this experiment we examined whether IC curvature mechanisms are selective for carrier contrast polarity. To do this, we used adaptors and tests that were either the same or opposite contrast polarity. If the SFAEs/SAAEs obtained with illusory contours are reduced when adaptor and test differ in contrast polarity, then IC curvature mechanisms must be tuned to contrast polarity. To provide a comparison with RCs, the effect of contrast polarity was also examined for two types of RCs: continuous contours (Fig. 1d) and contours consisting of Gaussian blobs (Fig. 1e) spaced at the same distance (0.5°) as the lines in the IC carrier. The reason for using contours made of Gaussian blobs is that they 'sample' the sine-wave contour similarly to that of the carrier in the ICs.

The contrast polarities of the RCs and the carrier lines of the ICs were either even-symmetric (Fig. 1c and the two upper contours in Fig. 1d) or odd-symmetric (Fig. 1a and the two lower contours in Fig. 1d). For ICs and continuous RCs there were six conditions: (a) adaptor and test both 'bright'; (b) adaptor and test both 'dark'; (c) adaptor 'bright' and test 'dark'; (d) adaptor 'dark' and test 'bright'; (e) adaptor and test both 'bright-dark', and (f) adaptor 'bright-dark' and test 'dark-bright'. Example ICs are shown in Fig. 1a and c. For RCs constructed from Gaussian blobs, we used isotropic Gabors with a spatial frequency of 0.001 c/deg and standard deviation of 0.05°. The spacing between the Gaussian blobs along the contour was 0.5°. Contours consisted of either 'bright', 'dark' or 'alternating bright and dark' Gaussian blobs, as shown in Fig. 1e. There were five conditions: (a) adaptor and test both 'bright'; (b) adaptor and test both 'dark'; (c) adaptor 'bright' and test 'dark'; (d) adaptor 'dark' and test 'bright'; (e) adaptor and test both made of alternating polarity Gaussian blobs.

In order to obtain an overall picture of the difference between the same and different contrast-polarity conditions, we normalized the after-effect for each contrast-polarity adaptor condition to the after-effect obtained using the corresponding same contrast-polarity adaptor/test condition, and separately for each observer. One can think of this measure as the amount of transfer of the after-effect in the different contrast-polarity condition. For example, 'white-to-dark' transfer for ICs (leftmost bar in Fig. 5a) was calculated as the after-effect obtained in the white-adaptor/dark-test condition normalized to the after-effect obtained in the same white adaptor/test condition.

Fig. 5 shows the results averaged across four observers for the SFAEs (left panels) and SAAEs (right panels): ICs (Fig. 5a, light gray bars), continuous RCs (Fig. 5b, dark gray bars) and RCs made of Gaussian blobs (Fig. 5c, black bars). A value of 1 (dashed lines in Fig. 5) indicates that the magnitude of the after-effect obtained in the different and same contrast-polarity adaptor/test conditions are similar. The results show: (i) similar sized after-effects obtained with IC adaptors/tests with opposite compared to same contrast-polarity (compare light gray bars with the dashed line in Fig. 5a); (ii) significantly lower after-effects with RC adaptors/tests (either continuous or made of Gaussian blobs) of opposite compared to same contrast-polarity (compare dark gray bars with the dashed line in Fig. 5b for continuous contours and compare black bars with the dashed line in Fig. 5c for contours made of Gaussian blobs); (iii) reduced SFAE but similar sized SAAE obtained with adaptor/test contours consisting of alternating-polarity Gaussian-blobs compared to same-polarity Gaussian-blobs (compare black bar labeled A/A with the dashed line in Fig. 5c). The large size and large error bar for the SFAE obtained with odd-symmetric RCs adaptor/test (last bar in the left panel in Fig. 5b) is due to the fact that one of the subjects (SW) did not show selectivity for contrast polarity with odd-symmetric RCs. Subject SW also showed no selectivity for contrast polarity with even-symmetric contours

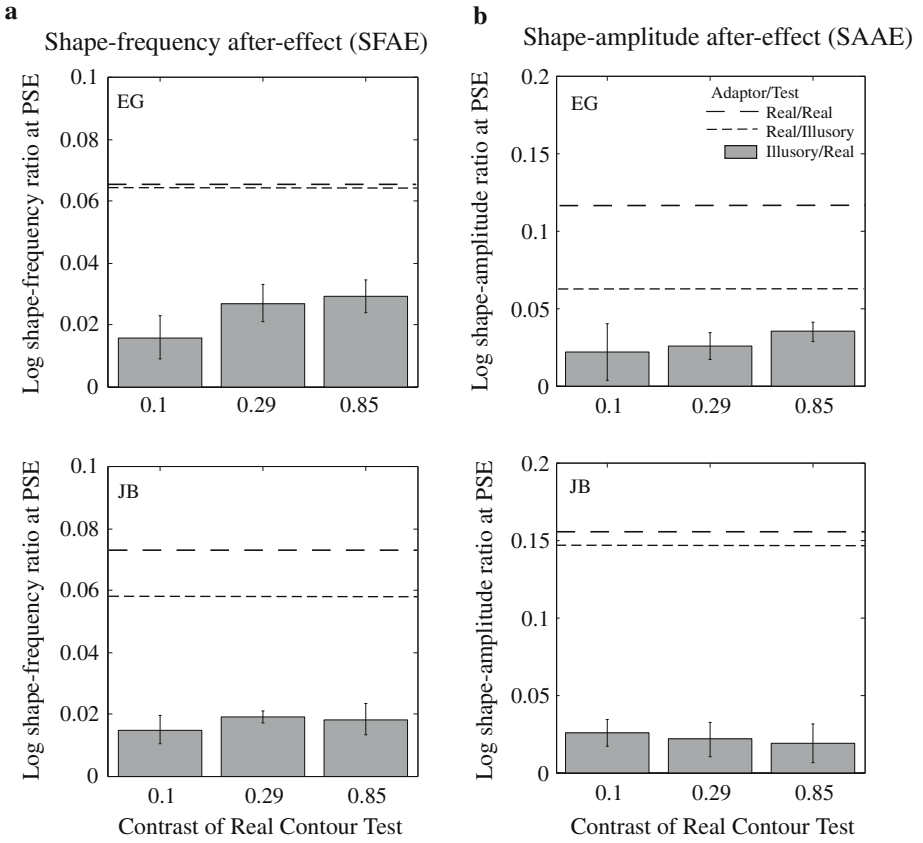

Fig. 4. (a) SFAEs and (b) SAAEs obtained with high contrast ICs adaptors and low-contrast RCs. For comparison, the dashed lines indicate the size of the after-effect obtained using the RC adaptor from the first experiment, thick dashed lines for the RC test and thin dashed lines for the IC test.

and showed lower SFAEs for same compared to opposite contrast-polarity odd-symmetric RCs. Fig. 5d plots the individual observer SFAEs obtained with odd-symmetric RCs for the same (light gray bars) and opposite (dark gray bars) contrast-polarities.

For each contour type (real and illusory), we tested whether the SFAEs/SAAEs for the same and opposite contrast-polarity adaptor/test conditions were significantly different. To do this we performed a two-factor within-subjects ANOVA (analysis of variance) with Phase (even-symmetric vs. odd-symmetric) and Contrast-Polarity (same vs. opposite) as factors on the non-normalized SFAE and SAAE. Same and opposite adaptor/test after-effects were not significantly different for ICs ($F(1, 1) = 0.11$; $p > 0.05$ for SFAE; $F(1, 1) = 1.33$; $p > 0.05$ for SAAE), were significantly different for continuous RCs ($F(1, 1) = 7.76$; $p < 0.05$ for SFAE, and $F(1, 1) = 48.33$; $p < 0.05$ for SAAE), and were significantly different for RCs made from Gaussian blobs ($F(1, 1) = 38.55$; $p < 0.05$ for SFAE, and $F(1, 1) = 57.96$; $p < 0.05$ for SAAE). The effect of Phase was found to be not significant for all types of contours (ICs: ($F(1, 2) = 0.02$; $p > 0.05$ for SFAE, and $F(1, 2) = 0.38$; $p > 0.05$ for SAAE; continuous RCs: $F(1, 2) = 0.17$; $p > 0.05$ for SFAE, and $F(1, 2) = 1.35$; $p > 0.05$ for SAAE; RCs made of Gaussian blobs: $F(1, 1) = 0.24$; $p > 0.05$ for SFAE, and $F(1, 1) = 0.01$; $p > 0.05$ for SAAE).

3.3. Experiment 3: effect of luminance-scale of the illusory-contour carrier

In this experiment we examined whether IC curvature mechanisms are selective for the luminance scale of the carrier. Adaptor and test contours were ICs constructed from line-grating carriers with odd-symmetric luminance profiles, of two standard deviations σ. The σs were $\sigma_f = 0.02°$ and $\sigma_c = 0.06°$, corresponding to 'fine' and 'coarse' scales. Example IC contours are shown in Fig. 5a for the coarse (left panel) and fine (right panel) carrier scales. Several adaptor/test combinations were tested: (i) adaptor/test with the same σ, either fine or coarse, and (ii) adaptor/test with different σ, either fine for adaptor and coarse for test, or vice versa. The contrast of both carriers was 0.85, but because the coarse-scale carriers might be stronger adaptors because of their greater contrast energy, we added a control condition in which the coarse-scale carrier contrast was reduced by a factor of 3 to 0.283. All the adaptor/test combinations mentioned in (i) and (ii) were tested again with low contrast coarse-scale and high contrast fine-scale carriers.

We again normalized the after-effect for each different σ adaptor/test condition to that of the corresponding same σ adaptor/test condition to provide a measure of the amount of transfer in the different σ condition. Fig. 6b shows normalized SFAEs (left panel) and SAAEs (right panel) for the different σ adaptor/test conditions for stimuli with a contrast of 0.85. Coarse-to-fine transfer is shown as light gray bars and fine-to-coarse transfer as dark gray bars. A value of 1 (dashed lines in Fig. 6b) indicates complete transfer. The results show some inter-subject variability. On average, there were larger SFAEs and SAAEs with coarse-scale adaptors and fine-scale tests for subjects EG and SW (compare light and dark gray bars) but this trend was reversed for subjects JB and MS in the SAAEs.

Fig. 6c shows SFAEs (left panel) and SAAEs (right panel) for all different σ adaptor-test combinations with low contrast (0.283) coarse-scale carriers and high contrast (0.85) fine-scale carriers normalized to the same σ adaptor-test conditions. The results show slightly bigger after-effects with low-contrast coarse-scale adaptors and high-contrast fine-scale tests than with high-contrast

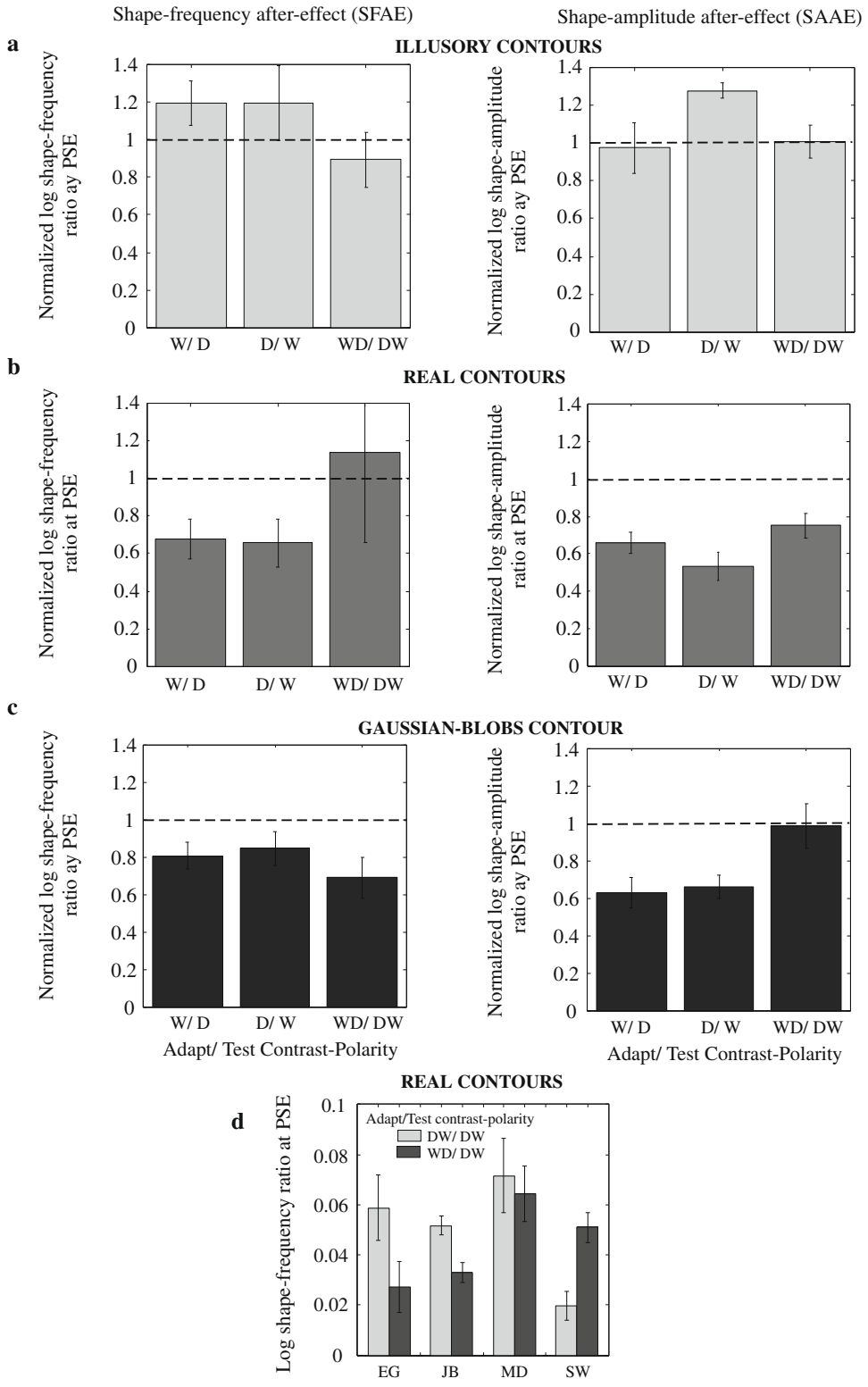

Fig. 5. Results for Experiment 2 investigating selectivity to luminance contrast polarity. Data are averaged across four observers for the SFAEs (left panels) and SAAEs (right panels). Different contrast-polarity adaptor/test conditions have been normalized to the same contrast-polarity adaptor/test condition. (a) ICs (light gray bars), (b) continuous RCs (dark gray bars) and (c) RCs made of Gaussian blobs (black bars). Same adaptor/test contrast-polarities are indicated by the dashed lines. A value of 1 (dashed lines) indicates that the magnitude of the after-effect obtained in the different and same conditions is the same. Different types of luminance profiles of the RCs and IC carriers are indicated as follows: 'W' – bright; 'D' – dark; 'WD' – bright-dark, 'DW' – dark-bright and 'A' – alternating bright and dark Gaussian-blobs. (d) SFAE obtained with odd-symmetric continuous RCs for the same (light gray bars) and opposite (dark gray bars) contrast-polarities adaptor and test for each observer.

fine-scale adaptor and low-contrast coarse-scale test (compare light gray with dark gray bars in Fig. 6c), except subject MS in the SFAE. These results indicate that irrespective of their contrast (either low 0.283 or high 0.85 contrast) ICs with coarse-scale carriers are slightly stronger adaptors than ICs with fine-scale carriers.

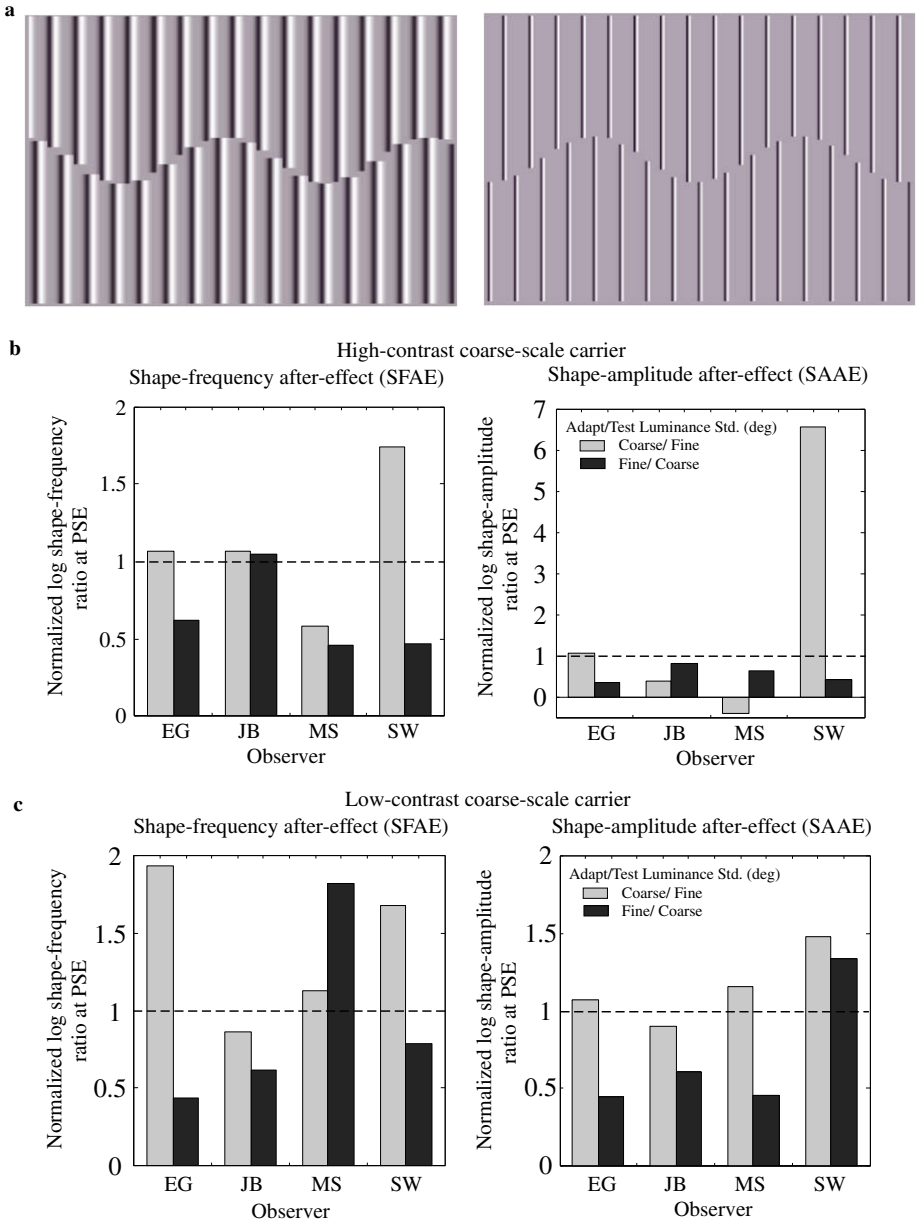

Fig. 6. (a) Example ICs constructed from odd-symmetric line-grating carriers whose luminance standard deviation σ was either 0.06° (left panel) or 0.02° (right panel), corresponding to fine and coarse scales. (b,c) results for Experiment 3: (b) SFAEs (left panel) and SAAEs (right panel), with same-contrast (0.85) for adaptor and test. Normalized coarse-to-fine carrier adaptor/test conditions are shown as light gray bars and fine-to-coarse carrier adaptor/test conditions are shown as dark gray bars. Dashed lines indicate same σ adaptor and test conditions. A value of 1 (dashed lines) indicates that the magnitude of the after-effect obtained in the different and same σ adaptor/test conditions are the same. (c) Normalized SFAEs (left panel) and SAAEs (right panel) for different σ adaptor/test conditions with low-contrast (0.283) coarse-scale carriers and high-contrast (0.85) fine-scale carriers.

We tested whether the SFAEs/SAAEs for the same and different luminance scale conditions were significantly different. To do so, we performed a two-factor within-subjects ANOVA (analysis of variance) on the non-normalized data obtained with low contrast (0.283) coarse-scale carriers and high contrast (0.85) fine-scale carriers, with Combination (same vs. opposite) and Adaptor-Scale (coarse vs. fine) as factors. The effect of Adaptor Scale was found to be significant for SAAE ($F(1, 1) = 12.80$; $p < 0.05$) but not the SFAE ($F(1, 1) = 1.40$; $p > 0.05$). There was no significant difference in either after-effect between the same and opposite adaptor-test combinations ($F(1, 1) = 0.27$; $p > 0.05$ for SFAE, and $F(1, 1) = 0.52$; $p > 0.05$ for SAAE). These results provide no compelling evidence that IC curvature mechanisms are tuned to the luminance scale of the carrier. However, ICs with coarse-scale carriers are slightly stronger adaptors than ICs with fine-scale carriers.

3.3.1. Control experiment 1: line-end orientation signals?

One reason why ICs with coarse-scale line carriers might be better adaptors than equal-energy fine-scale carriers is that they better stimulate first-order filters oriented at right-angles to the lines at their end-points. Line-end-sensitive filters might be pooled by a different type of 2nd-order mechanism from the one pooling filters oriented to the lines themselves, and contribute an additional after-effect. Since the carrier lines are odd-symmetric, the line ends would likely stimulate alternatively 'on' and 'off' sub-regions of horizontally-oriented receptive fields lying along the path of the

illusory contour. To test this possibility we performed an experiment using RC adaptors consisting of alternating 'bright' and 'dark' Gaussian blobs of coarse $\sigma = 0.06°$, as shown in Fig. 1e. There were three types of test contours: (i) RC adaptors consisting of alternating 'bright' and 'dark' Gaussian blobs of $\sigma = 0.06°$, (ii) ICs with fine-scale carrier lines ($\sigma = 0.02$), and (iii) ICs with coarse-scale carrier lines ($\sigma = 0.06$). If line-end signals are contributing to the after-effect from the IC adaptors with coarse-scale carriers (light gray bars in Fig. 6), then we should expect that Gaussian-blob RC adaptors produce similar after-effects in Gaussian-blob RC tests and coarse-scale-carrier IC tests, while a reduced after-effect with fine-scale-carrier IC tests.

Fig. 7 shows the SFAE (left panel) and SAAE (right panel), averaged across three observers, for Gaussian-blob RC adaptors with fine-scale-carrier (dark gray bars) and coarse-scale-carrier (black bars) ICs tests, this time normalized to the Gaussian-blob RC adaptor/test condition. The Gaussian-blob RC adaptor/test condition is shown as the light gray bars. The results show: (i) prominently reduced after-effects for Gaussian-blob RC adaptors combined with IC tests of either fine- or coarse-scale carriers (compare light gray bar with dark gray and black bars), and (ii) similar SFAEs and slightly smaller SAAEs for IC tests with coarse-scale compared to fine-scale carriers (compare dark gray bar with black bar). These results suggest that it is unlikely that the line-end orientation signals are contributing to the after-effects with coarse-scale carrier ICs.

3.3.2. Control experiment 2: coarse vs. fine-scale carrier coverage?

Another reason why ICs with coarse-scale line carriers might be better adaptors than those with fine-scale carriers is that they have greater coverage. To test this possibility we used fine-scale carrier ICs with the same coverage as coarse-scale-carrier ICs. The ICs with coarse-scale ($\sigma = 0.06°$) line-grating carriers had a duty cycle of 0.5° and the ICs with fine-scale ($\sigma = 0.02°$) line-grating carriers had a duty cycle of 0.166° – hence the ratio of σ and duty cycle, which is a measure of coverage, was the same for both types of carrier. Example IC contours are shown in Fig. 8a for fine (left panel) and coarse (right panel) carrier scales. All the adaptor/test combinations from the main experiment were tested again, that is: (i) adaptor/test with the same σ, either fine or coarse, and (ii) adaptor/test with different σ, either fine for adaptor and coarse for test, or vice versa. The contrast of both fine and coarse-scale carriers was 0.85. Only two observers participated in this experiment.

Fig. 8b shows normalized SFAEs (left panel) and SAAEs (right panel) for the different σ adaptor/test conditions. Coarse-to-fine transfer is shown as light gray bars and fine-to-coarse transfer as dark gray bars. A value of 1 (dashed lines in Fig. 8b) indicates complete transfer. The results show similar size SFAEs/SAAEs using coarse-scale adaptors and fine-scale tests and vice versa, indicating that if carrier coverage is equated the adaptive superiority of coarse-scale over fine-scale carrier ICs disappears.

3.4. Experiment 4: effect of carrier orientation

Here we examine whether IC curvature mechanisms are selective for the orientation of the line-grating carrier. We used odd-symmetric carrier lines oriented 20° to the left (Fig. 9a, left panel) or to the right (Fig. 9a, right panel) of vertical. We found that orientations greater than about 25° distorted the ICs since beyond 250 some carrier lines lay parallel to the tangent of the IC waveform at the d.c. Several adaptor and test conditions were tested: (i) adaptor and test with the same carrier orientation, either left or right oblique; (ii) adaptor and test with different carrier orientations, adaptor oriented to the left and test oriented to the right, and vice versa.

Fig. 9b shows the average across four observers for the normalized SFAE (left panel) and SAAE (right panel) for different orientation adaptor/test conditions (dark gray bars). The same orientation adaptor/test condition is shown as light gray bars. The results indicate that the after-effects appear similar for both same-orientation and different-orientation conditions.

A two-factor within-subjects ANOVA on the non-normalized data for SFAE and SAAE with Combination (same vs. different) and Orientation of adaptor (left vs. right) as factors showed that neither after-effect showed a significant difference between the same-orientation and different-orientation conditions ($F(1, 1) = 2.91$; $p > 0.05$ for SFAE, and $F(1, 1) = 1.98$; $p > 0.05$ for SAAE). The effect of Adaptor Orientation was also not significant for either the SFAE ($F(1, 1) = 0.04$, $p > 0.5$) or SAAE ($F(1, 1) = 0.00$, $p > 0.5$).

4. General discussion

We found a strong asymmetry in the transfer of SFAE/SAAE between real and illusory contour-shapes. When the adaptors were real contour (RC) shapes and the tests illusory contour (IC) shapes, the transfer was large: 1.4 for SFAE and 0.99 for SAAE. However, when the other way round, the transfer was relatively small: 0.31 for the SFAE and 0.35 for the SAAE. The asymmetry did not appear to be caused by a mismatch in contour saliency between adaptor and test. A similar asymmetry between ICs and RCs was reported for the tilt after-effect by Paradiso et al. (1989), though an earlier study by Smith and Over (1975) had found no such asymmetry and a later study by Berkley et al. (1994) found that the

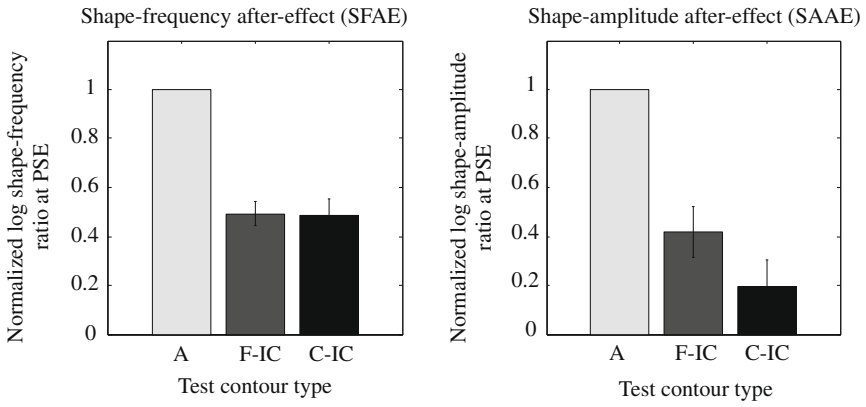

Fig. 7. SFAE (left panel) and SAAE (right panel), averaged across three observers, for Gaussian-blob RC adaptors with fine-scale-carrier (dark gray bars) and coarse-scale-carrier (black bars) ICs tests, normalized to the Gaussian-blob RC adaptor/test condition. The Gaussian-blob RC adaptor/test conditions are shown as the light gray bars.

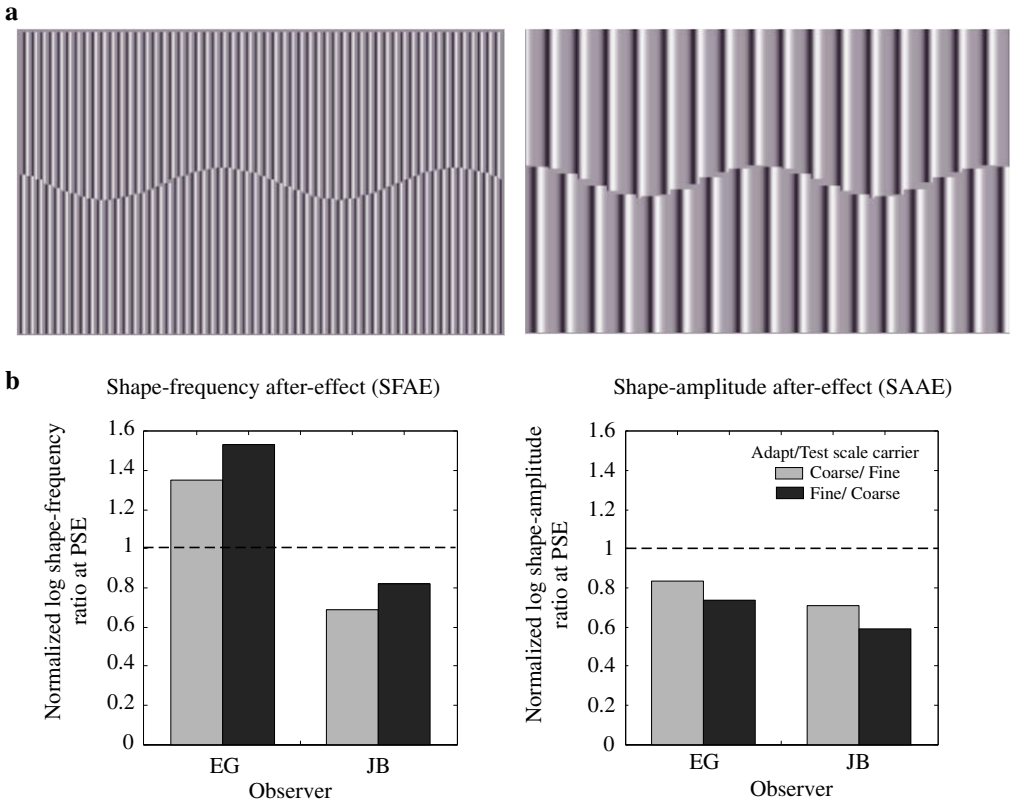

Fig. 8. (a) Example fine-scale ICs constructed from odd-symmetric line-grating carriers with duty cycle of 0.166° (left panel) and coarse-scale ICs constructed from line-grating carriers with duty cycle of 0.5° (right panel). (b) Normalized SFAEs (left panel) and SAAEs (right panel) for different σ and carrier duty-cycle adaptor/test conditions. The contrast was 0.85 for both coarse-scale (σ = 0.06°) and fine-scale (σ = 0.02°) carriers. Coarse-to-fine adaptor/test conditions are light gray bars and fine-to-coarse-scale adaptor/test conditions are dark gray bars. Dashed lines indicate same σ adaptor/test conditions. A value of 1 (dashed lines) indicates that the magnitude of the after-effect obtained in the different and same σ adaptor/test conditions is the same.

asymmetry almost disappeared when the RCs were degraded by noise. Paradiso et al. suggested that a possible reason why Smith and Over (1975) found no asymmetry was that their ICs had real-edge components. Paradiso et al. also argued that the asymmetry they found was not caused by the 'weakness' of their ICs, since the tilt after-effect obtained when both adaptor and test were ICs was relatively strong. Instead, Paradiso et al. argued that the asymmetry was a result of an imbalance in the population of neurons sensitive to RCs and ICs. Specifically, they argued, only a subset of the neurons sensitive to RCs were also sensitive to ICs. Their idea is consistent with neurophysiological studies showing that in V2, neurons responding to ICs constitute approximately 40% of the neural population that respond to RCs (von der Heydt et al., 1984; Peterhans, von der Heydt, & Baumgartner, 1986).

In our Experiment 1, the pronounced asymmetry in the transfer of the SFAE/SAAE between RC and IC curves could be explained similarly. That is, IC curves may be encoded by a sub-set of the mechanisms sensitive to RC curves. Thus when the adaptor was an RC and the test an IC, the adapted RC neurons included those sensitive to ICs, resulting in a large after-effect. However, when the adaptors were ICs and the tests RCs, only the sub-set of neurons responsive to ICs were adapted. Hence because the test was detected not only by the adapted IC neurons but also the unadapted RC neurons, the after-effect was relatively small. Moreover, the fact that the transfer of after-effect from RCs to ICs was greater or close to unity suggests that there are no neurons exclusively sensitive to IC curves. If there were, the test IC curves would be detected by at least some unadapted IC neurons, which would reduce the size of the after-effect. Thus in terms of the question we posed at the outset, namely whether RC shapes and IC shapes are processed by the same or different mechanisms, we conclude that the answer is neither one nor the other. We suggest that there are neurons that respond to both IC and RC curves, but that there are also neurons that respond only to RC curves. Put another way, IC curves are encoded by the same mechanisms as RC curves, but not entirely the other way around.

We found no compelling evidence that IC curvature mechanisms are selective for the contrast-polarity, luminance spatial scale and orientation of their line-grating carriers. These negative findings must be viewed in the light of the results obtained with RCs in the present study together with those using RCs in previous studies (Gheorghiu & Kingdom, 2006, 2007b), all showing that RC curvature mechanisms are selective to all the above properties. It would appear that IC curvature mechanisms display 'form-cue' invariance with regard to their carrier properties. This is an interesting finding as some classes of 2nd-order mechanism, for example those that detect spatiotemporal variations in contrast, are sensitive to contrast polarity (Badcock, Clifford, & Khuu, 2005; Chubb, Econopouly, & Landy, 1994; Malik & Perona, 1990; Motoyoshi & Kingdom, 2007; Rentschler, Hebner, & Caelli, 1988). The neurophysiological literature on the other hand shows that only a small minority of IC-responsive neurons in V2 are sensitive to contrast polarity (Baumann et al., 1997).

Illusory contours with coarse-scale carriers were shown to be somewhat more effective adaptors than those with fine-scale carriers when the number of carrier lines per image was the same. In one control experiment we showed that alternating Gaussian-blob contour adaptors produced smaller sized after-effects in coarse-scale-carrier compared to fine-scale-carrier IC tests, suggesting that 2nd order signals extracted from the endpoints of the

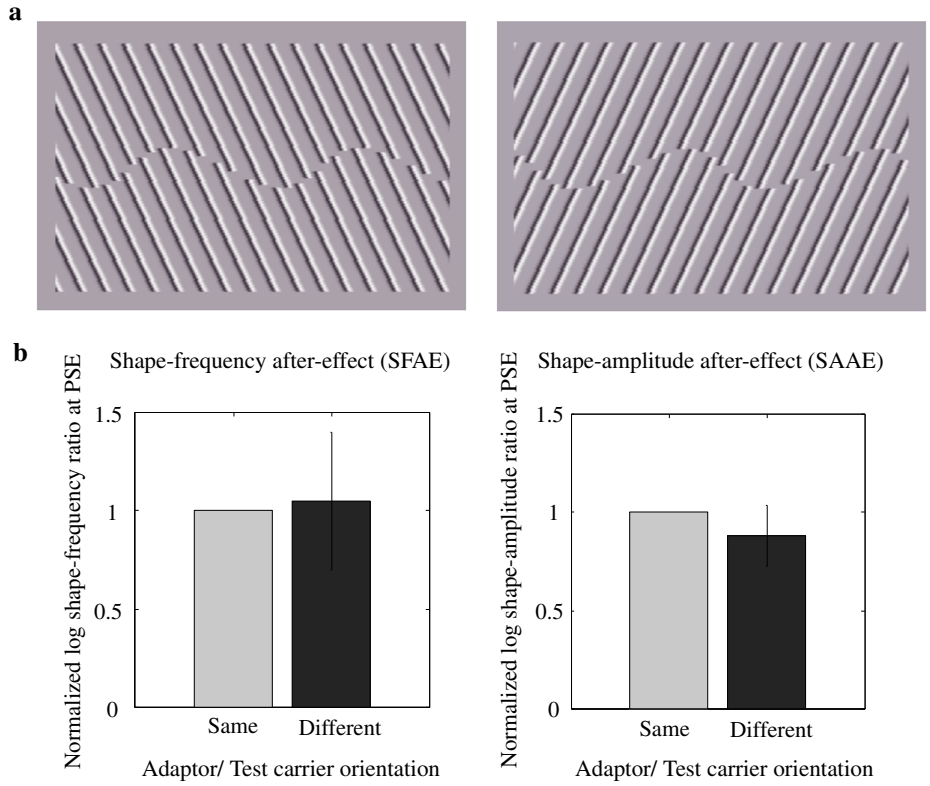

Fig. 9. (a) Example ICs constructed from odd-symmetric carrier lines oriented 20° to the right or to the left of vertical. (b) Results for Experiment 4, averaged across four observers, for the SFAE (left panel) and SAAE (right panel). Normalized different orientation adaptor/test conditions are shown as dark gray bars, same orientation adaptor/test condition as light gray bars.

coarse-scale carrier lines were unlikely to be the cause of the greater adaptive power. In another control experiment we showed that the superior adaptive power of the coarse-scale carrier ICs disappeared when the number of fine-scale carrier lines was increased to equal the coverage of the coarse-scale carrier lines. This suggests that in IC curvature mechanisms, the density of first-stage filters, meaning the number of filters per unit IC receptive-field area, is likely to be proportional to the square of filter spatial-frequency. This will help to maintain the response strengths of IC mechanisms over changes in viewing distance, a form of scale-invariance. Our finding that IC curvature mechanisms do not appear to be selective to carrier spatial frequency, which suggests that 1st-stage inputs are pooled across spatial-frequency, implies that the same IC mechanisms will respond across different viewing distances. The absence of selectivity to luminance spatial frequency however is at odds with neurophysiological studies showing that cat A18 neurons responding to ICs formed by abutting gratings exhibit selectivity to carrier spatial frequency (Song & Baker, 2006, 2007).

With regard to carrier orientation, we found that the introduction of a 40° difference between adaptor and test had no effect on the size of the after-effect, and although this is consistent with a lack of selectivity of IC curvature mechanisms to carrier orientation, the result must be treated with caution. It is possible that IC curvature mechanisms are tuned to carrier orientation, but broadly so, and that had we been able to employ a larger adaptor-test difference in carrier orientation we would have found some selectivity. Cat A18 neurons sensitive to ICs are indeed broadly tuned to carrier orientation (Song & Baker, 2006). In primates, a proportion of V2 neurons sensitive to ICs do show selectivity to carrier orientation, as well as selectivity to the orientation of the ICs (von der Heydt & Peterhans, 1989).

Acknowledgments

This research was supported by a Natural Sciences and Engineering Research Council of Canada (NSERC) Grant # OGP01217130 given to F.K.

References

Badcock, D. R., Clifford, C. W., & Khuu, S. K. (2005). Interactions between luminance and contrast signals in global form detection. *Vision Research, 45*(7), 881–889.
Baumann, R., van der Zwan, R., & Peterhans, E. (1997). Figure-ground segregation of contours: A neural mechanism in the visual cortex of the alert monkey. *European Journal of Neurophysiology, 9*(6), 1290–1303.
Berkley, M. A., Debruyn, B., & Orban, G. (1994). Illusory, motion, and luminance-defined contours interact in the human visual system. *Vision Research, 34*(2), 209–216.
Chubb, C., Econopouly, J., & Landy, M. S. (1994). Histogram contrast analysis and the visual segregation of IID textures. *Journal of the Optical Society of America A – Optics Image Science and Vision, 11*(9), 2350–2374.
Dresp, B., Salvano-Pardieu, V., & Bonnet, C. (1996). Illusory form with inducers of opposite contrast polarity: Evidence for multistage integration. *Perception & Psychophysics, 58*(1), 111–124.
Ffytche, D. H., & Zeki, S. (1996). Brain activity related to the perception of illusory contours. *NeuroImage, 3*(2), 104–108.
Gheorghiu, E., & Kingdom, F. A. A. (2006). Luminance-contrast properties of contour-shape processing revealed through the shape-frequency after-effect. *Vision Research, 46*(21), 3603–3615.
Gheorghiu, E., & Kingdom, F. A. A. (2007a). The spatial feature underlying the shape-frequency and shape-amplitude after-effects. *Vision Research, 47*(6), 834–844.
Gheorghiu, E., & Kingdom, F. A. A. (2007b). Chromatic tuning of contour-shape mechanisms revealed through the shape-frequency and shape-amplitude after-effects. *Vision Research, 47*(14), 1935–1949.
Gheorghiu, E., & Kingdom, F. A. A. (2008). Spatial properties of curvature-encoding mechanisms revealed through the shape-frequency and shape-amplitude after-effects. *Vision Research, 48*(9), 1107–1124.
Gheorghiu, E., & Kingdom, F. A. A. (2009). Multiplication in curvature processing. *Journal of Vision, 9*(2), 23. 1–17.
Gheorghiu, E., Kingdom, F. A. A., Thai, M-T., & Sampasivam, L. (2009). Binocular properties of curvature-encoding mechanisms revealed through two shape after-effects. *Vision Research, 49*(14), 1765–1774.

Greene, H. H., & Brown, J. M. (1997). Spatial interaction with real and gap-induced illusory lines in vernier acuity. *Vision Research, 37*(5), 598–604.
Grosof, D. H., Shapley, R. M., & Hawken, M. J. (1993). Macaque V1 neuronscan signal 'illusory' contours. *Nature, 365*(6446), 550–552.
Von Grunau, M. W. (1979). The involvement of illusory contours in stroboscopic motion. *Perception & Psychophysics, 25*(3), 205–208.
Halpern, D. F., Salzman, B., Harrison, W., & Widaman, K. (1983). The multiple determination of illusory contours: 2. An empirical investigation. *Perception, 12*(3), 293–303.
Hancock, S., & Peirce, J. W. (2008). Selective mechanisms for simple contours revealed by compound adaption. *Journal of Vision, 8*(7): 11, 1–10.
He, Z. J., & Ooi, T. L. (1998). Illusory-contour formation affected by luminance contrast-polarity. *Perception, 27*(3), 313–335.
von der Heydt, R., & Peterhans, E. (1989). Mechanisms of contour perception in monkey visual cortex. I. Lines of pattern discontinuity. *Journal of Neuroscience, 9*(5), 1731–1748.
von der Heydt, R., Peterhans, E., & Baumgartner, G. (1984). Illusory contours and cortical neuron responses. *Science, 224*(4654), 1260–1262.
Hirsch, J., DeLaPaz, R. L., Relkin, N. R., Victor, J., Kim, L., Li, T., et al. (1995). Illusory contours activate specific regions in human visual cortex: Evidence from functional magnetic resonance imaging. *Proceedings of the National Academy of Sciences of the United States of America, 92*(4), 6469–6473.
Huxlin, K. R., Saunders, R. C., Marchionini, D., Pham, H. A., & Merigan, W. H. (2000). Perceptual deficits after lesions of inferotemporal cortex in macaques. *Cerebral Cortex, 10*(7), 671–683.
Lee, T. S., & Nguyen, M. (2001). Dynamics of subjective contour formation in the early visual cortex. *Proceedings of the National Academy of Sciences of the United States of America, 98*(4), 1907–1911.
Lesher, G. W., & Mingolla, E. (1993). The role of edges and line-ends in illusory contour formation. *Vision Research, 33*(16), 2253–2270.
Malik, J., & Perona, P. (1990). Preattentive texture discrimination with early vision mechanisms. *Journal of the Optical Society of America A, 7*(5), 923–932.
Merigan, W. H. (1996). Basic visual capacities and shape discrimination after lesions of extrastriate are V4 in macaques. *Visual Neuroscience, 13*(1), 51–60.
Mendola, J. D., Dale, A. M., Fischl, B., Liu, A. K., & Tootell, R. B. (1999). The representation of illusory and real contours in human cortical visual areas revealed by functional magnetic resonance imaging. *Journal of Neuroscience, 19*(19), 8560–8572.
Montaser-Kouhsari, L., Landy, M. S., Heeger, D. J., & Larsson, J. (2007). Orientation-selective adaptation to illusory contours in human visual cortex. *Journal of Neuroscience, 27*(9), 2186–2195.
Motoyoshi, I., & Kingdom, F. A. A. (2007). Differential roles of contrast polarity reveal two streams of second-order visual processing. *Vision Research, 47*, 2047–2054.
Paradiso, M. A., Shimojo, S., & Nakayama, K. (1989). Subjective contours, tilt aftereffects, and visual cortical organization. *Vision Research, 29*(9), 1205–1213.
Parks, T. E. (1980). The subjective brightness of illusory figures: Is stratification a factor? *Perception, 9*(3), 361–363.
Peterhans, E., & von der Heydt, R. (1989). Mechanisms of contour perception in monkey visual cortex II Contours bridging gaps. *Journal of Neuroscience, 9*(5), 1749–1763.
Peterhans, E., & Heitger, F. (2001). Simulation of neuronal responses defing depth order and contrast polarity at illusory contours in monkey area V2. *Journal of Computational Neuroscience, 10*(2), 195–211.
Peterhans, E., von der Heydt, R., & Baumgartner, G. (1986). Neuronal responses to illusory contour stimuli reveal stages of visual cortical processing. In J. D. Pettigrew, K. J. Sanderson, & W. R. Levick (Eds.), *Visual neuroscience* (pp. 343–351). Cambridge: Cambridge University Press.
Petry, S., Harbeck, A., Conway, J., & Levey, J. (1983). Stimulus determinants of brightness and distinctness of subjective contours. *Perception & Psychophysics, 34*(2), 169–174.
Prazdny, K. (1983). Illusory-contours are not caused by simultaneous brightness contrast. *Perception and Psychophysics, 34*(4), 403–404.
Ramachandran, V. S. (1986). Capture of stereopsis and apparent motion by illusory contours. *Perception and Psychophysics, 39*(5), 361–373.
Rentschler, I., Hebner, M., & Caelli, T. (1988). On the discrimination of compound Gabor signals and textures. *Vision Research, 28*, 279–291.
Sary, G., Chadaide, Z., Tompa, T., Koteles, K., Kovacs, G., & Benedek, G. (2007). Illusory shape representation in the monkey inferior temporal cortex. *European Journal of Neuroscience, 25*(8), 2558–2564.
Smith, A. T., & Over, R. (1975). Tilt aftereffects with subjective contours. *Nature, 257*(5527), 581–582.
Smith, A. T., & Over, R. (1977). Orientation masking and the tilt illusion with subjective contours. *Perception, 6*(4), 441–447.
Smith, A. T., & Over, R. (1979). Motion aftereffect with subjective contours. *Perception & Psychophysics, 25*(2), 95–98.
Song, Y., & Baker, C. L. Jr., (2006). Neural mechanisms mediating responses to abutting gratings: Luminance edges vs illusory contours. *Visual Neuroscience, 23*(2), 181–199.
Song, Y., & Baker, C. L. Jr., (2007). Neuronal response of texture- and contrast-defined boundaries in early visual cortex. *Visual Neuroscience, 24*(1), 65–77.
Soriano, M., Spillman, L., & Bach, M. (1996). The abutting grating illusion. *Vision Research, 36*(1), 109–116.
Tyler, C. W. (1975). Stereoscopic tilt and size aftereffects. *Perception, 4*, 187–192.
Vogels, R., & Orban, G. A. (1987). Illusory contour orientation discrimination. *Vision Research, 27*(3), 453–467.
De Weerd, P., Desimone, R., & Ungerleider, L. G. (1996). Cue-dependent deficits in grating orientation discrimination after V4 lesions in macaques. *Visual Neuroscience, 13*(3), 529–538.
Wilson, H. R., & Richards, W. A. (1992). Curvature and separation discrimination at texture boundaries. *Journal of the Optical Society of America A, 9*(10), 1653–1662.
Van der Zwan, R., & Wenderoth, P. (1995). Mechanisms of purely subjective contour tilt aftereffects. *Vision Research, 35*(18), 2547–2557.